CHEMISTRY OF MATERIALS

ARTICLE

pubs.acs.org/cm

Ultrathin Selective Molecularly Imprinted Polymer Microdots Obtained by Evanescent Wave Photopolymerization

Yannick Fuchs,[†] Ana V. Linares,[†] Andrew G. Mayes,[‡] Karsten Haupt,[*,†] and Olivier Soppera[*,§]

[†]Compiègne University of Technology, UMR CNRS 6022, BP20529, Compiègne, 60205, France

[‡]School of Chemistry, University of East Anglia, Norwich NR4 7TJ, United Kingdom

[§]Mulhouse Institute for Material Sciences, CNRS LRC 7228, BP2488, Mulhouse, 68057, France

Supporting Information

ABSTRACT: The fabrication of ultrathin selective molecularly imprinted polymer (MIP) microdots using polymerization by evanescent waves (PEW) is demonstrated for the first time. A specific prepolymerization mixture exhibiting suitable photosentivity at 405 nm was developed, containing in particular the visible-light photoinitiator bis(2,4,6-trimethylbenzoyl)-phenylphosphineoxide. PEW allows for nanometric resolution of the MIP dots in the z-scale. Within a few seconds, it is possible to generate molecularly imprinted microdots with sub-100 nm thickness. The amino acid *Z*-(L)-phenylalanine was used as model imprinting template, and the fluorescent dansyl-phenylalanine was employed as a fluorescently labeled derivative for the recognition tests. The MIP microdots showed specific molecular recognition for (L)-phenylalanine derivatives and were able to discriminate dansyl-(L)-phenylalanine from dansyl-(D)-phenylalanine.

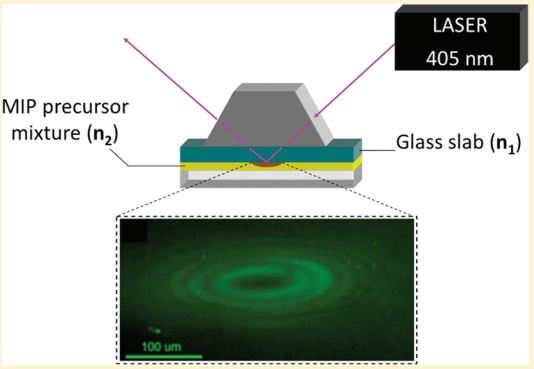

KEYWORDS: photopolymerization, evanescent wave, molecularly imprinted polymer, synthetic receptor, microstructuring, molecular recognition

INTRODUCTION

Molecularly imprinted polymers (MIPs) are biomimetic synthetic receptors capable of binding target molecules with high specificity.[1−3] Initially, a template molecule self-assembles with functional monomers in an excess of cross-linking monomers, to form a complex through noncovalent interactions. After polymerization, the template is removed, and the resulting material exhibits a 3-dimensional structure, complementary in size, shape, and position of the functional groups to the template molecule. Owing to this molecular memory, imprinted polymers are able to recognize and bind target molecules and thus act as synthetic receptors mimicking natural biological receptors, for example in chemical sensors and biochips. The integration of imprinted polymers into sensors and similar devices in a suitable form such as thin films, micro and nanopatterns, is the main challenge of practical sensor development and requires processes for microfabricating MIPs in two- and three-dimensional patterns, possibly with additional multiscale structuring. In this context, photolithographic methods are of great interest. Using photopolymerization, the MIP can be synthesized in situ, which is far more difficult with thermal polymerization, still the method of choice for bulk MIP synthesis. Indeed, photoinduced radical polymerization is associated with a number of advantages, such as fast reaction, room temperature polymerization, and spatial control of polymerization. Several lithographic techniques have previously been used for MIP synthesis, such as microstereolithography,[4,5] mid-infrared laser pulse (the only example of a localized thermal polymerization),[6] UV-mask projection lithography,[7] microcontact printing,[8] soft lithography,[9] or fountain pen micro or nanolithography.[10,11] One very interesting option that has not been used so far for MIP synthesis is the optical near field. Near-field photolithography makes it possible to reach a resolution below the diffraction limit, and has been shown to be a powerful method for nanoscale photofabrication of polymers.[12] More particularly, polymerization by evanescent wave (PEW) has been demonstrated to be one possible method for reducing the size of polymeric features in the z-dimension, since the evanescent wave generated by total internal reflection of a light beam extends only a few hundreds of nanometers (depending on the wavelength) into the polymerization medium. With specific optical arrangements using interfering lasers, nanofabrication in the *x*-*y*-dimensions is also possible.[13−15] Here, we report for first time the fabrication of ultrathin molecularly imprinted polymer microdots using PEW as photolithographic method. The interest of this route is to provide a simple and rapid method to implement MIP dots on a substrate with multiscale structuring: (i) microscale resolution for the lateral size of the dots, (ii) nanoscale thickness (<100 nm), (iii) nanoscale porosity to gain access to molecularly imprinted binding sites, and (iv) molecular imprinting. The key-point was to develop a specific photosensitive MIP recipe that

Received: April 6, 2011
Revised: July 5, 2011
Published: July 29, 2011

is compatible with PEW. The possibility of initiating the polymerization with visible light is of particular interest since to date all the reports on the photopolymerization of MIPs used UV light. We describe here the photopolymerization of reproducible polymeric micropatterns in a few seconds, exhibiting thicknesses of only tens of nanometers, and specific molecular recognition of dansyl-(L)-phenylalanine (dansyl-(L)-Phe), a fluorescent amino acid derivative used as a model target.

EXPERIMENTAL SECTION

Materials. Methacrylic acid (MAA, inhibited with 250 ppm MEHQ), 4-vinylpyridine (4-VPy), ethylenglycol dimethacrylate (EGDMA, inhibited with 100 ppm MEHQ), and dansyl-(L)-phenylalanine (dansyl-(L)-Phe) were purchased from Sigma-Aldrich. *N*-(carbobenzyloxy)-(L)-phenylalanine (*Z*-(L)-Phe) was obtained from Fluka. Dansyl-(D)-phenylalanine (dansyl-(D)-Phe) was purchased from Biosynthan GmbH (Germany) and bis(2,4,6-trimethylbenzoyl)-phenylphosphineoxide (Irgacure819) was generously provided by Ciba Specialty Chemicals (France). 4-VPy was vacuum-distilled before use and all other monomers were employed without further purification. The solvents used were anhydrous and of analytical grade.

MIP Precursors Solutions. The MIP mixture was prepared using a 1:4:4:40 molar ratio between the template *Z*-(L)-Phe, the functional monomer MAA, the functional monomer 4-VPy and the cross-linking monomer EGDMA. The amount of photoinitiator Irgacure819 used was either 0.05 mol % or 1.00 mol % relative to the mole number of polymerizable groups present in the system. Acetonitrile was used as porogenic solvent, and the volume ratio between the porogen and the monomers was 6:5. Nonimprinted control polymers (NIPs) were prepared from the same precursors but in the absence of the template molecule. Because of their high sensitivity to actinic light, the prepolymerization mixtures were kept in the dark until use, and not longer than 5 days.

Preparation of Bulk Polymers. Four milliliters glass vials (1 cm in diameter) containing the polymer precursors solutions were sealed with a septum cap covered with Parafilm, and the mixtures were purged with nitrogen for 2 min. Polymerization was carried-out by placing the vials on a daylight light box equipped with 18 W standard fluorescent tubes. After 1 h of irradiation, the polymers were recovered by breaking the glass vials. The monoliths were first manually crushed in a mortar and then transferred to microcentrifuge tubes, suspended in methanol and finely ground with 2.8 mm-diameter ceramic beads in a Precellys 24 homogenizer (Bertin Technologies, Montigny le Bretonneux, France). The polymer particles were then washed three times using 10 mL of a methanol/acetic acid (9:1) mixture, followed by two washes with 10 mL of ethanol and a final wash using 10 mL of methanol. Each washing step was performed during 1 h in centrifuge tubes under agitation at room temperature. Particles were separated from solvent using centrifugation at 10 000 rpm at 10 °C for 20 min. Finally, the polymers were dried under vacuum overnight. To confirm the efficient extraction of the template, a chemically identical MIP was synthesized using a chlorinated template analogue (for its structure, see Supporting Information, Figure SI.1), allowing for the use of energy dispersive X-ray spectroscopy. The spectra recorded before and after template extraction (see Supporting Information, Figure SI.2) confirm the absence of template in the final MIP by the absence of the chlorine peak. A nonimprinted control polymer (NIP) was synthesized under identical conditions but in the absence of the template.

Characterization of Bulk Polymers. Increasing amounts of polymer ranging from 0 to 9 mg were suspended in acetonitrile in microcentrifuge tubes and incubated with a fixed concentration of dansyl-Phe (L or D enantiomers). The final volume was 1 mL for all samples. The microcentrifuge tubes were protected from light and placed on a rotation wheel overnight. The samples were then centrifuged at 14 000 rpm at room temperature for 15 min to sediment the polymer particles. The fluorescence intensity of 700 μL of the supernatant was measured using a Cary Eclipse fluorescence spectrometer from Varian (λ_{EX} 340 nm/λ_{EM} 485 nm). The percentage of bound dansyl-Phe was calculated as follows: % bound dansyl-Phe = $(FI_0 - FI_{sample})/FI_0 \times 100$, where FI_0 is the fluorescence intensity of an initial solution of dansyl-Phe in acetonitrile without polymer, and FI_{sample} is the fluorescence intensity of the supernatants after incubation with the polymers.

Fabrication of Ultrathin Polymer Microdots. A 405 nm laser diode was used as actinic light source. High refractive index glass slabs and prisms (n_1 = 1.62) were used. The refractive index of the photosensitive polymer precursors solutions was measured with a refractometer to be n_2 = 1.41. According to these values the critical angle θ_c was 70°. To avoid any residual reflection at the interface between the prism and the substrate, index matching solution (Cargille Laboratories, U.S.A.) with n_{match} = 1.62 was employed. Ten microliters of the photosensitive polymer precursor solutions were cast on a standard glass microscope slide and covered with the high-index glass slab. Approximately 200 μL of index matching solution were uniformly spread on the top of the high-index glass slab, and the prism was placed over it. The whole system was then adjusted on an *x-y* table, and the polymerization performed by irradiation at a power of 22.5 mW (spot size : 1 mm × 1.5 mm). The laser power was systematically measured and adjusted prior to each experiment by using a real-time single channel power meter (Coherent Power Max USB-PS19Q) at the prism output. Polymerization times ranged from 10 to 90 s, depending on the photoinitiator concentration. After polymerization, the standard and high index glass slabs were carefully separated, and unreacted monomers were removed from the surface of the high-index slab by sonication in anhydrous dimethylsulfoxide (DMSO) for a few seconds. Finally, the slab was rinsed with ethanol and dried in an air stream. The *Z*-(L)-Phe template was extracted from the polymer microdots by placing the high index glass slab with the microdots face-down in a methanol/acetic acid solution (9:1) for 1 h under gentle agitation. This washing process was repeated three times, followed by two rinses with ethanol and one with methanol.

Analysis of Ultrathin Polymer Microdots. The polymer microdots were incubated for 2 h in 5 mL of a dansyl-Phe solution in acetonitrile, under gentle agitation and protected from light. After incubation, the microdots were rinsed with 5 mL of acetonitrile and dried prior to fluorescence microscopy measurements. The fluorescence of the ultrathin polymer microdots was measured using a Leica DMI6000 B fluorescence microscope, equipped with a 360 nm excitation/470 nm emission filter cube for the detection of dansyl labels. The optical microscope parameters such as exposure time, gain, and intensity were kept constant during the acquisition of the fluorescent images of the MIP and NIP microdots. The fluorescence intensity values were then quantified using the software ImageJ (public domain, http://rsb.info.nih.gov/ij/), and were corrected for the fluorescent background of the support. The fluorescent signals of dots incubated with dansyl-(D)-Phe were corrected using a factor of 1.197 determined through fluorescence spectroscopy measurements of several dansyl-(L)-Phe and dansyl-(D)-Phe solutions in acetonitrile of exactly the same concentrations.

RESULTS AND DISCUSSION

Choice of the Visible-Light Photoinitiator. The first objective of this work was to develop a molecularly imprinted polymer photopolymerizable under visible-light. As a model template, we chose *Z*-(L)-Phe for the possibility of later using the fluorescent derivative dansyl-(L)-Phe for binding studies. Ramström et al. reported in an early paper that molecular imprinting of N-protected (L)-phenylalanine derivatives benefits from the association of basic and acidic functional monomers, due to the presence

Scheme 1. Radical Decomposition Scheme of Bis[2,4,6-trimethylbenzoyl]-phenylphosphineoxide

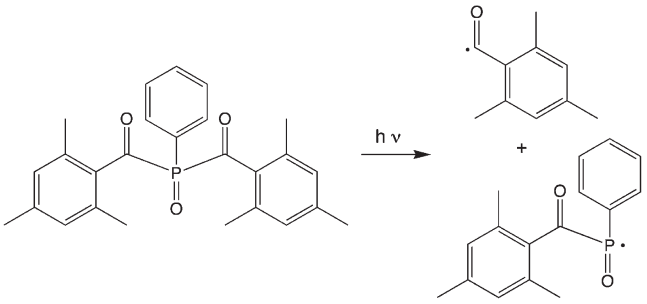

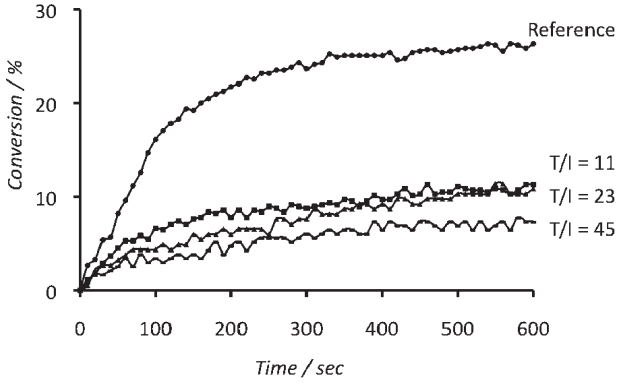

Figure 1. Kinetics of photopolymerization: Conversion of different precursors mixtures as a function of time, measured by RT-FTIR. Conversion = $(Abs_0 - Abs_t)/Abs_0$. T/I represents the molar ratio between molecular template and photoinitiator.

of both an acidic function (interacting with the basic 4-VPy) and hydrogen bonding moieties (interacting with MAA).[16] In the present study we have therefore used a combination of 4-VPy and MAA as functional monomers, together with EGDMA as the cross-linking monomer. The choice of the photoinitiator is crucial since photosensitivity of the MIP precursors solutions derives from this species. Potential interactions between photoinitiator and the other components of the mixture have to be avoided so as not to interfere with the polymerization reaction or with the template-monomer complex. After screening a number of visible-light photoinitiators, we finally selected bis(2,4,6-trimethylbenzoyl)-phenylphosphineoxide. Its photoinduced radical decomposition is shown in Scheme 1. This acylphosphine oxide based dye shows the distinct advantage of undergoing a fast photolysis under light exposure, leading to very reactive radicals.[17] Its strong absorption in the UV−vis range (300−450 nm) and its high reactivity toward acrylates and methacrylates make it very suitable for the photopolymerization of MIPs, allowing for polymerization at 405 nm.[18] An additional advantage of using visible-light photopolymerization for MIP synthesis is that it avoids exposure to UV light that could possibly provoke a degradation of sensitive template molecules.

Influence of the Template and Photoinitiator Concentration on Polymerization Kinetics. To assess a possible impact of the template molecule on the polymerization kinetics, the polymerization was followed by real-time Fourier transform infrared spectroscopy (RT-FTIR). A reference mixture was

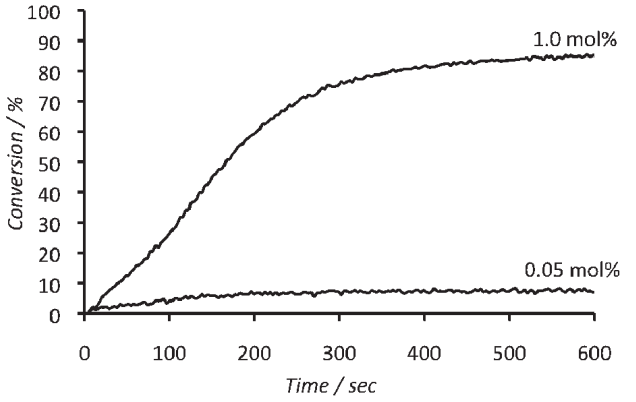

Figure 2. Effect of the photoinitiator concentration on the polymerization reaction conversion of two different precursors mixtures (without template). Concentration of photoinitiator is expressed as mol % relative to the total number of moles of polymerizable groups (irradiation intensity: 10 $mW.cm^{-2}$).

prepared consisting of 4-VPy, MAA, EGDMA, 0.05 mol % of photoinitiator, and acetonitrile. In addition, three MIP precursors solutions were prepared by adding to the reference mixture *Z*-(L)-Phe at molar ratios of 11, 23, and 45 with respect to the photoinitiator. The solutions were then cast between a KBr disk and a polypropylene film and irradiated with a 405 nm laser diode at 12.3 $mW.cm^{-2}$. This intensity is much lower than the one produced by the evanescent wave during polymerization, but is more convenient to elucidate differences in polymerization kinetics of the different mixtures. The polymerization kinetics was deduced by monitoring the relative disappearance of the methacrylic groups, characterized by a band in the IR spectrum at 1637 cm^{-1}. Figure 1 shows the progress of the polymerization reaction as a function of the irradiation time for the four different precursor mixtures. The reference sample, prepared without molecular template, exhibits the fastest polymerization kinetics. The maximum of conversion (about 25%) is reached after 600 s of irradiation. This final conversion is relatively low, which can be explained by the low light intensity and low photoinitiator concentration. However, it should be emphasized that even with such a limited conversion, the polymer was firmly attached to the substrate. When adding *Z*-(L)-Phe at a 11:1 ratio with respect to the photoinitiator, the polymerization kinetic is highly affected because after 600 s of irradiation, the conversion ratio is only about 12%. With increasing template concentration, the rate of polymerization as well as the maximum conversion decrease further, though slightly. Hence, it is obvious that the presence of *Z*-(L)-Phe in the precursor mixture has an effect on the polymerization kinetics. One potential explanation may be a proton exchange of the primary radicals issued from the photolysis of the photoinitiator with the template. The resulting radical may be inactive toward methacrylates, which may account for the relative loss of efficiency. However, despite the low polymerization conversion measured, polymerization could be carried out and MIPs were fabricated from this precursor solution.

As described in the literature, the photosensitivity of the photopolymerization mixture is directly linked to the concentration of photoinitiator in the system.[19] For microstructuring applications, a high photoinitiator concentration is favorable since the resulting fast polymerization kinetic avoids problems related to the diffusion of reactive species and the stability of the

dx.doi.org/10.1021/cm2009829 |*Chem. Mater.* 2011, 23, 3645–3651

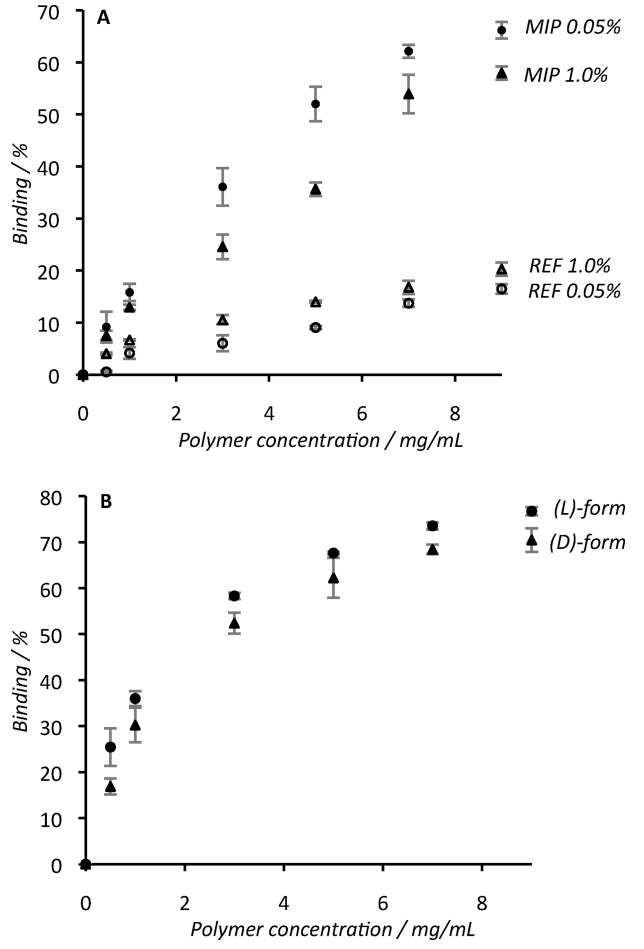

Figure 3. A: Binding isotherms of dansyl-(L)-Phe adsorption to MIPs and NIPs synthesized with different photoinitiator concentrations, 0.05 mol % (circles) and 1 mol % (triangles) with respect to the number of polymerizable groups. Full symbols: MIP, open symbols: non-imprinted controls. B: Normalized binding isotherms of 1 μM dansyl-(L)-Phe or dansyl-(D)-Phe to a MIP imprinted with *Z*-(L)-Phe. The experiments were done in triplicate, and the error bars represent the standard deviation.

optical setup (vibrations, light source fluctuation).[20] On the other hand, for molecular imprinting, slower kinetics are preferred to favor the phase separation between the growing polymer and the solvent, inducing a good porosity in the material and leading to a better accessibility of the binding sites in the MIP for the target molecules. Thus, a compromise needs to be found. We have therefore studied the effect of the photoinitiator concentration on the polymerization kinetics of nonimprinted polymers. The results are shown in Figure 2. They illustrate the high dependency of the polymerization rate on the photoinitiator concentration at a light intensity of 10 mW.cm^{-2}. When using a high photoinitiator concentration of 1.0 mol % relative to the number of polymerizable groups in the system, the maximum conversion ratio is about 80% after 400 s. When using a 20 times lower photoinitiator concentration of 0.05 mol %, the maximum conversion ratio is less than 10% after 400 s. Hence, regarding these results, the low photopolymerization rate observed in Figure 1 appears to be a direct consequence of the low photoinitiator concentration, and this parameter can be used to adjust the photosensitivity of the pre-polymerization mixture.

Molecular Recognition Capacity of an Imprinted Bulk Polymer. Prior to ultrathin MIP microdot fabrication by PEW, bulk MIPs and NIPs of the same composition were evaluated. This was done as a control to confirm that the specific conditions and ingredients necessary for PEW were compatible with molecular imprinting. Bulk MIPs were prepared using the two different concentrations of photoinitiator mentioned in the previous part, 1.0 mol % and 0.05 mol % with respect to the number of polymerizable groups. Control polymers prepared in the absence of template were tested in parallel. The MIPs were imprinted with *Z*-(L)-Phe and binding assays were performed by incubation with dansyl-(L)-Phe, a fluorescent derivative. After sedimenting the particles by centrifugation, the fluorescence in the supernatant was quantified. Figure 3A represents the binding isotherms. It shows an appreciable imprinting effect since considerably more binding of the fluorescent ligand to the MIPs than to the controls is observed. The MIP synthesized with the lower initiator content shows better binding than that with 1 mol % initiator. The same is true for the imprinting factor (IF = binding to the MIP/binding to the control). With the MIP synthesized with 0.05 mol % initiator, the imprinting factor is 17 at a polymer concentration of 0.5 mg/mL, whereas with the MIP synthesized with 1 mol % initiator, the IF is only 2. With the MIP synthesized with 0.05 mol % initiator, with increasing polymer concentrations, the nonspecific binding increases and lower IF are obtained (for example, IF = 6 at 5 mg/mL). With the MIP synthesized with 1 mol % initiator, the IF varies only little over the polymer concentration range tested. The effect of polymerization kinetics on the binding properties of MIP has already been studied previously in our group in the context of spin-coated MIP films.[21] We found that rapid polymerization rates can prevent the phase separation of the growing polymer network from the porogenic solvent, leading to a nonporous material and preventing access of the template molecule to the specific binding sites. The results shown in Figure 3 point in the same direction, better imprinting factors and binding capacities being obtained at lower initiator concentration and thus slower polymerization rates. To test for selectivity, the binding of dansyl-(D)-Phe to a MIP imprinted with *Z*-(L)-Phe (synthesized with 0.05 mol % initiator) was also studied (Figure 3B). As can be seen, the MIP shows a preference for the L enantiomer, which seems to confirm the selectivity of the MIP. However, this selectivity is small, which is probably due to the limited structural similarity between *Z*-Phe and dansyl-Phe, indicating the need of 'perfect' binding sites to distinguish the enantiomers.

Fabrication of Ultrathin MIP Microdots by PEW. Evanescent waves were generated under total internal reflection conditions at the interface between a high index prism and the MIP precursor mixture. The two media have different refractive indices (n_1 and n_2 for glass and precursor mixture, respectively), with $n_1 > n_2$.

As shown in Figure 4, when a light beam propagates through a high refractive index medium (n_1) and reflects at the interface with a medium of lower refractive index (n_2) with an angle (θ) bigger than the so-called critical angle (θ_c), the incident beam totally reflects, creating an evanescent field from the interface n_1/n_2 into the low refractive index medium (n_2). This evanescent wave is then able to initiate polymerization of the MIP precursor mixture. The critical angle θ_c is calculated as follows:

$$\theta_c = \arcsin\left(\frac{n_2}{n_1}\right) \quad (1)$$

dx.doi.org/10.1021/cm2009829 |*Chem. Mater.* 2011, 23, 3645–3651

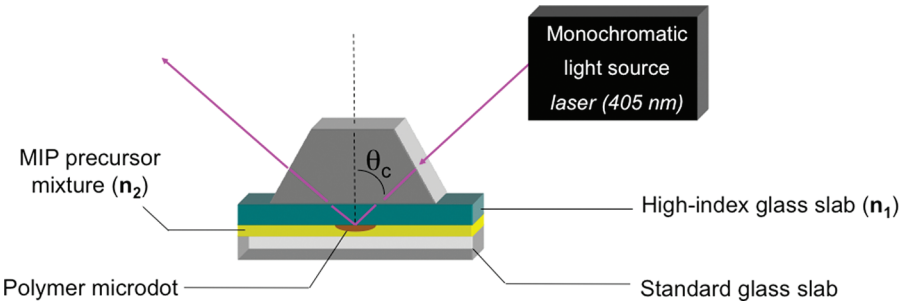

Figure 4. Schematic drawing of the setup used for polymerization of MIP microdots by evanescent wave.

The intensity of the evanescent field $I_{(z)}$ decays exponentially with the distance across the low-index medium as given by eq 2:

$$I_{(Z)} = I_0 \exp(-2\gamma z) \quad (2)$$

Where I_0 is the intensity of the incident beam and γ the decay rate defined by eq 3:

$$\gamma = \frac{2\pi}{\lambda}\sqrt{(n_1 \sin(\theta))^2 - {n_2}^2} \quad (3)$$

The characteristic penetration depth of the evanescent field is given by $1/(2\gamma)$ and represents the thickness of the theoretical layer where the evanescent field is confined. Consequently, the characteristic penetration depth is proportional to the thickness of the polymerized layer e that can be predicted by eq 4, assuming polymerization of the material at values of I_0 greater than a threshold value E_{th}.

$$e = \frac{1}{2\gamma}\ln\left(\frac{I_0 \times t_e}{E_{th}}\right) \quad (4)$$

This logarithmic relationship of the polymer thickness with the beam intensity at the interface and the exposure time t_e has been experimentally confirmed for a limited range of incident intensities and for films with thickness smaller than 500 nm.[22]

The limitation of the spatial extent of the polymerization reaction is not only linked to the confinement of the electromagnetic wave. It is also due to a nonlinear response of the photopolymer characterized by a polymerization threshold. The polymerization threshold is linked to the chemical nature of the photoinitiator and monomers, to the presence of inhibitors (such as oxygen), and to diffusion parameters.[13,23]

Ultrathin molecularly imprinted polymer microdots were fabricated using evanescent wave photopolymerization at 405 nm using both low (0.05 mol %) and high (1 mol %) initiator concentrations. The diode power was set at 22.5 mW (spot size : 1 mm × 1.5 mm) and kept constant. The mixture containing 1 mol % of initiator was polymerized for 15 s, while the one containing 0.05 mol % of initiator was polymerized for 90 s. The microdots were imaged by optical microscopy, fluorescence microscopy, and white light interferometric microscopy. In interferometric microscopy, a flat surface gives rise to parallel fringes with equal distance between two consecutive fringes. An object with a height of x nm induces a deviation of the straight fringes from $(x/(\lambda/2)) \times 100\%$. From the observation of the fringe deviation, the height of the dots can be deduced. Typical examples of microdots are shown in Figure 5. With $\lambda = 546$ nm, the resulting maximum height of the polymer microdots was evaluated to be about 60 nm for the MIP and 45 nm for the NIP, demonstrating that this method allows fabrication of ultrathin polymer films. It has to be noticed that Newton's rings are clearly visible on the microscopy images. They are due to diffraction of the laser beam. In the present case, this was not considered a problem to demonstrate the concept of PEW of the MIP. Moreover, such effects can be eliminated by introducing a spatial filter in the optical pathway. The synthesis of these MIP microdots was very reproducible if all experimental conditions were kept constant, the variation in thickness between dots being less than 10%.

The surface morphology of the microdots at the nanoscale was analyzed using AFM in contact mode (for images see Supporting Information, Figure SI.3). Microdots prepared with a high concentration of photoinitiator exhibit macropores (roughness about 23 nm), whereas microdots fabricated using 0.05 mol % of photoinitiator show, in addition to some macropores, a large number of homogeneously distributed mesopores (roughness about 10 nm). This difference can be attributed to the difference in polymerization rate in both systems: fast polymerization prevents the phase separation between polymer and porogenic solvent and thus leads to lower porosity, whereas slow polymerization allows the generation of additional mesoporosity.[21] This is in accordance with the binding characteristics of the bulk polymers described above.

Molecular Recognition Capacity of Ultrathin MIP Microdots Synthesized by PEW. The specificity and selectivity of the MIP microdots photopolymerized in the evanescent field geometry were evaluated. Three ultrathin MIP and three NIP microdots were polymerized using 0.05 mol % of photoinitiator and 90 s irradiation. After elution of the template from the MIP, the microdots were incubated in a 1 μM dansyl-(L)-Phe solution in acetonitrile for 2 h at 21 °C, under gentle agitation in the dark. After incubation, the dots were rinsed by quickly dipping into acetonitrile and dried under a stream of N_2. The fluorescence signal emitted by the microdots was then measured using fluorescence microscopy. The microscopy images were analyzed using the ImageJ software to quantify the fluorescence signal. The results in Figure 6 show that the MIP dots imprinted with Z-(L)-Phe bind more dansyl-(L)-Phe than the non-imprinted control dots, which confirms specific binding of the target to the MIP and thus molecular imprinting. The imprinting factor (IF = 2) is smaller than the one obtained with the best bulk polymers, which is probably due to some non-specific binding to the underlying glass substrate in the case of the microdots, and to the different inner morphologies of the bulk and thin film materials. Binding studies were also performed with the opposite enantiomer, dansyl-(D)-Phe using the same dots. Similar binding to the MIP and control dots was observed, which indicates some degree of enantiospecificity and thus selectivity of the MIP.

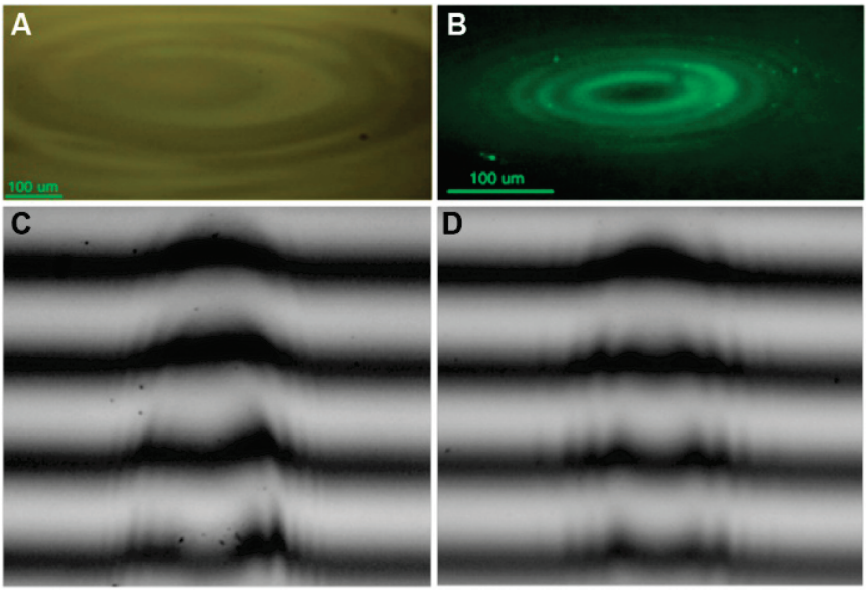

Figure 5. (A) Optical microscope image (20×) of a MIP microdot; (B) fluorescence microscope image (20×) of a MIP microdot; interferential microscopy images of (C) a MIP microdot and (D) a NIP microdot (for interferential microscopy, microdots were covered with 10 nm of gold by vacuum deposition).

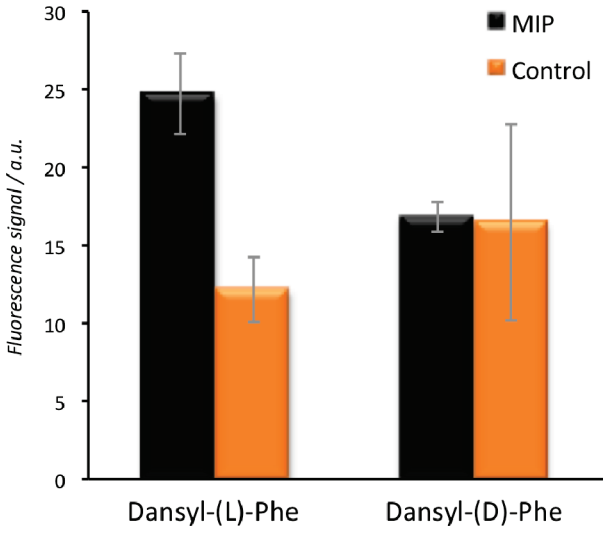

Figure 6. Normalized fluorescence signal of ultrathin MIP microdots measured by fluorescence microscopy after a 2 h incubation in 1 μM dansyl-(L)-Phe or dansyl-(D)-Phe in acetonitrile. The measurements were made using three different MIP dots and three different NIP dots, and represent mean values. The error bars represent the standard deviation. The dots were regenerated after each binding experiment and reused.

CONCLUSION

We have developed a new method of molecularly imprinted polymer synthesis at the micro and nanoscales, using photopolymerization in the optical near field. The use of evanescent wave photopolymerization aided by a visible light-sensitive photoinitiator makes it possible to fabricate well controlled molecularly imprinted microstructures in only tens of seconds. By adjusting the photosensitive formulation, the MIP microdot morphology (size and porosity) can be optimized and the polymer thickness tuned to less than 100 nm. Moreover, these MIP microdots showed specific binding of the fluorescent template derivative dansyl-(L)-Phe and exhibited molecular selectivity between the L and D enantiomers of the amino acid derivative.

ASSOCIATED CONTENT

Supporting Information. Figure SI.1: Molecular structure of the template derivative *N*-(2-chlorobenzyloxycarbonyl)-(*R*)-β2-homophenylalanine used in the template extraction efficiency study; Figure SI.2: Energy Dispersive X-ray Spectroscopy results of a bulk MIP imprinted with N-(2-chlorobenzyloxycarbonyl)-(*R*)-β2-homophenylalanine (A) Prior to template extraction and (B) After washing for template extraction; Figure SI.3: AFM topography image of ultrathin molecularly imprinted polymer microdots. This material is available free of charge via the Internet at http://pubs.acs.org.

AUTHOR INFORMATION

Corresponding Author

*E-mail: karsten.haupt@utc.fr (K.H.), olivier.soppera@uha.fr (O.S.).

ACKNOWLEDGMENT

We gratefully acknowledge financial support from the European Union (Marie Curie Research Training Network NASCENT, Grant MRTN-CT-2006-33873, and co-funding of analytical equipment), from the French National Research Agency (ANR – Project HOLOSENSE, ANR-08-BLAN-0236-02), and from the Regional Council of Picardy (France).

REFERENCES

(1) Haupt, K. *Anal. Chem.* **2003**, *75*, 376.
(2) Zimmerman, S.; Lemcoff, N. *Chem. Commun.* **2004**, *2004*, 5.
(3) Haupt, K.; Mosbach, K. *Chem. Rev* **2000**, *100*, 2495.

(4) Bertsch, A.; Jezequel, J.; Andre, J. *J. Photochem. Photobiol., A* **1997**, *107*, 275.
(5) Conrad, I.; Nishimura, P.; Aherne, D.; Schwartz, B.; Wu, D.; Fang, N.; Zhang, X.; Roberts, M.; Shea, K. *Adv. Mater.* **2003**, *15*, 1541.
(6) Henry, O.; Piletsky, S.; Cullen, D. *Biosens. Bioelectron.* **2008**, *23*, 1769.
(7) Guillon, S.; Lemaire, R.; Linares, A.; Haupt, K.; Ayela, C. *Lab Chip* **2009**, *9*, 2987.
(8) Voicu, R.; Faid, K.; Farah, A. A.; Bensebaa, F.; Barjovanu, R.; Py, C.; Tao, Y. *Langmuir* **2007**, *23*, 5452.
(9) Lalo, H.; Ayela, C.; Dague, E.; Vieu, C.; Haupt, K. *Lab Chip* **2010**, *10*, 1316.
(10) Vandevelde, F.; Loechlé, T.; Ayela, C.; Bergaud, C.; Nicu, L.; Haupt, K. *Langmuir* **2007**, *23*, 6490.
(11) Belmont, A.; Sokuler, M.; Haupt, K.; Gheber, L. *Appl. Phys. Lett.* **2007**, *90*, 193101.
(12) Deeb, C.; Bachelot, R.; Plain, J.; Baudrion, A. L.; Jradi, S.; Bouhelier, A.; Soppera, O.; Jain, P. K.; Huang, L.; Ecoffet, C.; Balan, L.; Royer, P. *ACS Nano* **2010**, *4*, 4579.
(13) Ecoffet, C.; Espanet, A.; Lougnot, D. *Adv. Mater.* **1998**, *10*, 411.
(14) Triger, C.; Ecoffet, C.; Lougnot, D. *J. Phys. D: Appl. Phys.* **2003**, *36*, 2553.
(15) Soppera, O.; Jradi, S.; Ecoffet, C.; Lougnot *Proc. SPIE* **2007**, *6647*, 6647OI.
(16) Ramstroem, O.; Andersson, L.; Mosbach, K. *J. Org. Chem.* **1993**, *58*, 7562.
(17) Decker, C.; Zahouily, K.; Decker, D.; Nguyen, T.; Viet, T. *Polymer* **2001**, *42*, 7551.
(18) Szablan, Z.; Junkers, T.; Koo, S.; Lovestead, T.; Davis, T.; Stenzel, M.; Barner-Kowollik, C. *Macromolecules* **2007**, *40*, 6820.
(19) Decker, C.; Moussa, K. *Polym. Mat. Sci. Eng* **1986**, *55*, 552.
(20) Soppera, O.; Jradi, S.; Lougnot, D. *J. Polym. Sci., Part A: Polym. Chem.* **2008**, *46*, 3783.
(21) Schmidt, R.; Haupt, K. *Chem. Mater.* **2005**, *17*, 1007.
(22) Espanet, A.; Ecoffet, C.; Lougnot, D. *J. Polym. Sci., Part A: Polym. Chem.* **1999**, *37*, 2075.
(23) Croutxé-Barghorn, C.; Soppera, O.; Lougnot, D. *Eur. Phys. J.: Appl. Phys.* **2001**, *13*, 31.